Sustainable Cities and Society 36 (2018) 225–236

Contents lists available at ScienceDirect

Sustainable Cities and Society

journal homepage: www.elsevier.com/locate/scs

Projected changes to extreme wind and snow environmental loads for buildings and infrastructure across Canada

Dae Il Jeong*, Laxmi Sushama

Centre ESCER (Étude et Simulation du Climat à l'Échelle Régionale), Université du Québec à, Montréal, Montreal, Canada

ARTICLE INFO

Keywords:
Building codes
Canada
Climate change
Extremes
Snow load
Wind pressure

ABSTRACT

Wind and snow are major environmental loads that are often considered in the design of buildings and infrastructure. To ensure safety of existing structures and to develop guidelines for future developments, it is important to evaluate how these design loads will be impacted by the anticipated climate change. This study evaluates projected changes to selected return levels of wind speed and snow water equivalent (SWE) and associated wind pressure and ground snow loads across Canada for the future 2071–2100 period. Canadian Regional Climate Model (CRCM5) simulations driven by two Global Climate Models (GCMs) for two future emission scenarios are used. The CRCM5 projections suggest some increases in the future 50-year return levels of wind speed and pressure, mainly due to changes in inter-annual variability of annual maximum wind speed, particularly for the central and eastern regions. As for SWE loads, results suggest general decreases for southern Canada and increases for northern Canada in the 50-year return levels. However, the projections, particularly for wind loads, vary considerably with the driving GCM and the emission scenario, suggesting that larger ensembles including more RCMs and driving GCMs will be required to better quantify uncertainties to support development of climate-resilient design standards and codes.

1. Introduction

Environmental loads should be taken into consideration in the design of buildings and infrastructure to ensure successful performance and reliability. Wind and snow loads are the major environmental loads considered in the National Building Code of Canada (NBCC) (NRCC, 2015). The design loads are based on selected return levels obtained from annual maximum time series of the respective environmental load. However, according to the Intergovernmental Panel on Climate Change (IPCC, 2012), the frequency, severity, duration, and timing of extreme events including those related to wind and snow can change in a future warmer climate. These changes might have significant implications for existing buildings and infrastructure, which were designed based on environmental loads estimated from historical observations (Steenbergen, Koster, & Geurts, 2012).

The NBCC defines wind load as the external pressure or suction due to wind on the surface of a building or structure (NRCC, 2015). The NBCC (NRCC, 2015) specifies the design wind pressure for various return periods for selected locations across Canada based on the design wind speed estimated from the Gumbel distribution fitted to the annual maximum series of hourly mean wind speed. Several studies have looked at the historical trends in the near-surface mean and extreme wind speeds, and they reported general decreasing trends across the globe (McVicar et al., 2012; Romanić, Ćurić, Jovičić, & Lompar, 2015). Vautard, Cattiaux, Yiou, Thépaut, and Ciais (2010) showed that surface wind speeds declined by 5–15% over almost all continental areas in the northern mid-latitude for the 1979–2008 period. Over Canada, Wan, Wang and Swail (2010) reported significant decreases in 10-m hourly wind speed for western Canada and most parts of southern Canada for all four seasons, while significant increases are reported for central Canadian Arctic for all seasons and for Maritimes during spring and autumn. Hundecha, St-Hilaire, Ouarda, El Adlouni, and Gachon (2008) showed increases in annual maximum wind speeds in a regional reanalysis over southern Maritimes based on 1979–2003 data. Holt and Wang (2012), Romanić, Hangan, and Ćurić (2016) and Romanić, Rasouli, and Hangan (2017) showed some positive trends in near surface wind speed for the northern US states (near the Canadian border), Great Lakes region, and an urban region in Toronto, primarily due to the increasing trend in westerly wind. Global Climate Models (GCMs), coupling atmosphere, land, ocean and sea-ice components of the earth system, are the most comprehensive tools used to assess climate-change projections. However, projected changes to extreme winds based on GCMs are less clear over Canada due to limited studies as well as the difficulties associated with their coarse resolution (IPCC, 2012). To

* Corresponding author at: Centre ESCER, Université du Québec à Montréal, 201 Ave. President-Kennedy, Montreal, Quebec H2X3Y7, Canada.
E-mail address: jeong@sca.uqam.ca (D.I. Jeong).

http://dx.doi.org/10.1016/j.scs.2017.10.004
Received 20 December 2016; Received in revised form 30 June 2017; Accepted 5 October 2017
Available online 05 November 2017
2210-6707/ © 2017 Elsevier Ltd. All rights reserved.

address such constraints to some extent, Cheng, Li, Li, Auld, and Fu (2012) and Cheng, Lopes, Fu, and Huang (2014) developed a statistical downscaling model to generate future wind gust from eight GCM simulations and showed that frequency of wind gust events could increase across Canada by the end of the 21 century. Regional climate models (RCMs) are used to add physical details to GCM simulations and to investigate climate processes and extremes at fine spatial scales. However, detailed studies on regional-scale projections of extreme wind speeds based on RCM simulations and associated changes in design wind pressure of buildings/structures are not yet attempted for Canada.

Snow loading is specified to consider snow accumulation on roofs or any other building surface, and ground snow load is used as the reference to estimate roof snow loads in Canada (NRCC, 2015). The total snow load in the NBCC consists of two components: ground snow load and an associated rain load. The ground snow load is based on the 50-year return level estimated from the Gumbel distribution fitted to the annual maximum daily snow depth. The associated rain load is to consider wet snow conditions, which is constrained not to exceed the design ground snow load. Hong and Ye (2014) analyzed extreme snow load using observed snow depth data from 549 stations and suggested spatially interpolated maps for the ground snow loads for Canada. Peacock (2012) investigated projected changes to snow depth over North America using the Community Climate System Model, version 4 (CCSM4) global simulations and showed a general decrease across Canada and significant decrease over mountainous western Canada in January-March mean snow depth for the future (2080–2099) period with respect to current (1980–1999) period. On the other hand, Huziy et al. (2013) showed no significant changes in winter (DJF) mean snow water equivalent (SWE) over northeastern Canada for future 2041–2070 period with respect to the current 1970–1999 period, based on an ensemble of the Canadian RCM simulations. However, Canada-wide analyses of extreme ground snow, based on high-resolution RCMs, are still limited. Projected changes to rain-on-snow (ROS) events for the future 2041–2070 period with respect to the current 1976–2005 period over North America based on RCM simulations were studied by Jeong and Sushama (2017). Their study showed general increases in ROS frequency during November to March for most regions of Canada for the future period, due to an increase in the rainfall frequency with warmer air temperatures in the future. The rain component is not covered in the present study as it is usually smaller than 10% of the ground snow load component as reported in NBCC (Hong & Ye, 2014).

The main purpose of this study is to evaluate projected changes to the 50-year return levels of wind speed and ground snow and the associated wind pressure and ground snow load for the future 2071–2100 period, with respect to the current 1981–2010 period over Canada, using four different simulations from the fifth-generation Canadian Regional Climate Model (CRCM5). The CRCM5 is based on the numerical weather prediction model of Environment and Climate Change Canada (ECCC). The CRCM5 simulations considered in this study are driven by two GCMs (i.e., Canadian Earth System Model 2 (CanESM2) and Max-Planck-Institut Earth System Model (MPI-ESM)) for Representative Concentration Pathways (RCP) 4.5 and 8.5 scenarios. The RCPs are a set of greenhouse gas concentration trajectories designed to support research on impacts to climate change, and the 4.5 and 8.5 scenarios correspond to radiative forcings of 4.5 and 8.5 W/m^2 by the end of the 21 st century compared to pre-industrial values, respectively (IPCC, 2013). As wind direction is important in determining wind pressure and the dynamic effects on buildings and structures, projected changes to wind direction of annual maximum wind speed are also assessed. Additionally, projected changes to winter snow density and probable dates of annual maximum ground snow are also evaluated in this study.

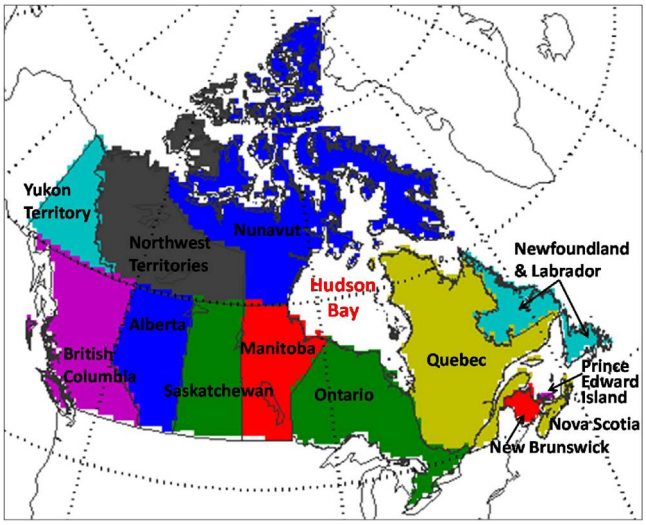

Fig. 1. Provines and Territories of Canada.

2. Model simulations and observed datasets

2.1. CRCM5 simulations

The CRCM5 is based on the Global Environmental Multiscale (GEM) model (Côté et al., 1998), and the physical parameterizations in CRCM5 are similar to those in GEM, except for the land surface and the radiation schemes. Radiation is parameterized by Correlated K solar and terrestrial radiation of Li and Barker (2005). Canadian Land Surface Scheme (CLASS) 3.5 (Verseghy, 2009, 2012) is employed for the land part. This version of CLASS includes prognostic equations for energy and water conservation for a user-defined number of soil layers and thermally and hydrologically distinct snowpack where applicable (treated as an additional variable-depth soil layer). The thermal budget is performed over all soil layers but the hydrological budget calculations are performed only for layers above bedrock. An explicit vegetation canopy has its own energy and water balance with prognostic variables for canopy temperature and water storage.

The experimental domain of CRCM5 covers whole of North America and neighbouring oceans at 0.44° resolution. This study is however focused on the Canadian landmass only (Fig. 1). The atmospheric lateral boundary conditions are obtained from the ECMWF (European Centre for Medium-Range Weather Forecasts) gridded ERA-Interim reanalysis dataset at 0.75° resolution (Dee et al., 2011), the CanESM2 simulated dataset (Arora et al., 2011), and the MPI-ESM simulated data (Giorgetta et al., 2013). The simulation driven by the ERA-Interim reanalysis (CRCM5-ERA hereafter) for the 1981–2014 period is used for the evaluation of CRCM5. The CRCM5 simulations, driven by CanESM2 and MPI-ESM for the 1981–2014 period used in this study, are referred to as CRCM5-CanHist and CRCM5-MPIHist. These simulations are used to evaluate boundary forcing errors, when compared to the reference ERA-driven simulations (Jeong, Sushama, Khaliq, & Roy, 2014; Jeong, Sushama, Diro, & Khaliq, 2016; Jeong, Sushama et al., 2016). In addition to the above mentioned simulations, four CRCM5 simulations driven by CanESM2 and MPI-ESM for the RCP4.5 and RCP8.5 pathways, for the 2015–2100 period are also considered for the analysis of projected changes. For presentation convenience, these simulations are named as CRCM5-CanRCP4.5, CRCM5-CanRCP8.5, CRCM5-MPIRCP4.5, and CRCM5-MPIRCP8.5 to reflect both the boundary forcing dataset and emission pathway considered. To quantify projected changes, the simulations for the future 2071–2100 period are compared with that for the 1981–2010 period.

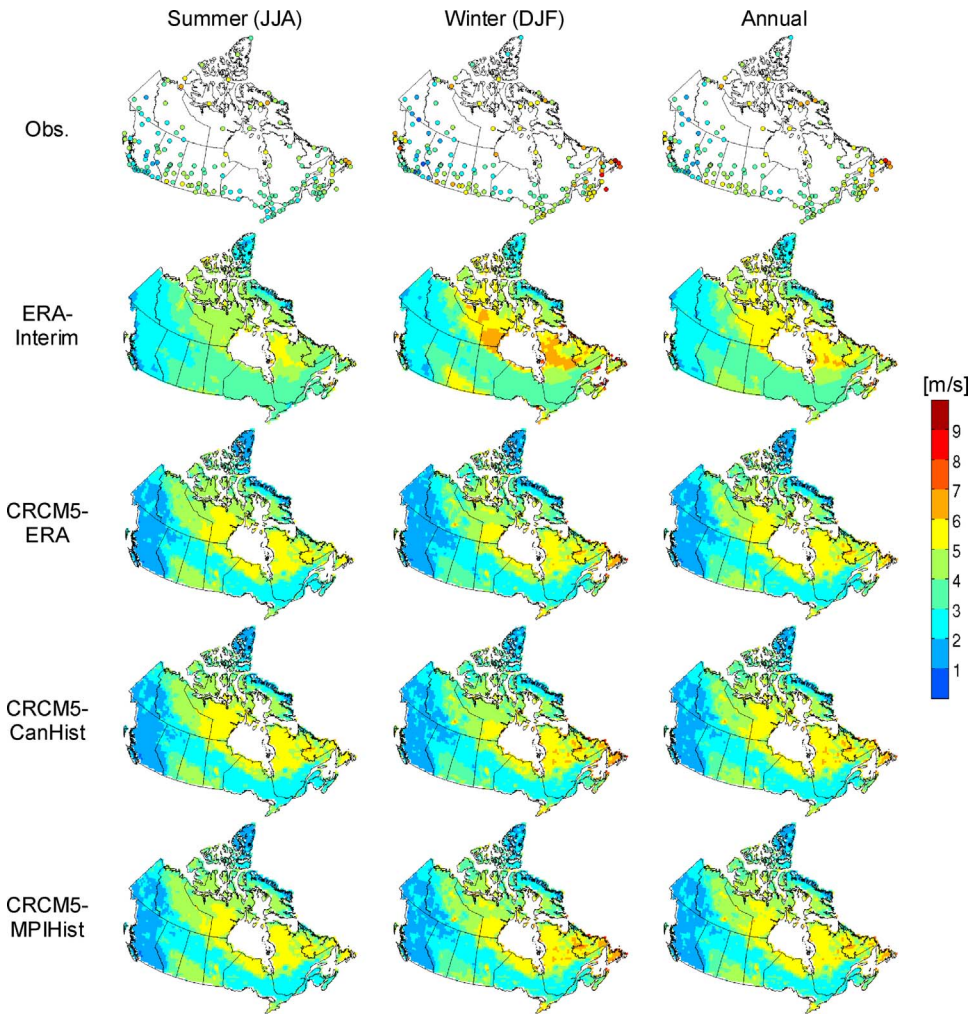

Fig. 2. Summer (JJA), winter (DJF), and annual mean wind speed from observations, ERA-Interim reanalysis, and CRCM5 simulations (i.e., CRCM5-ERA, −CanHist, and −MPIHist) for 1981–2010 period.

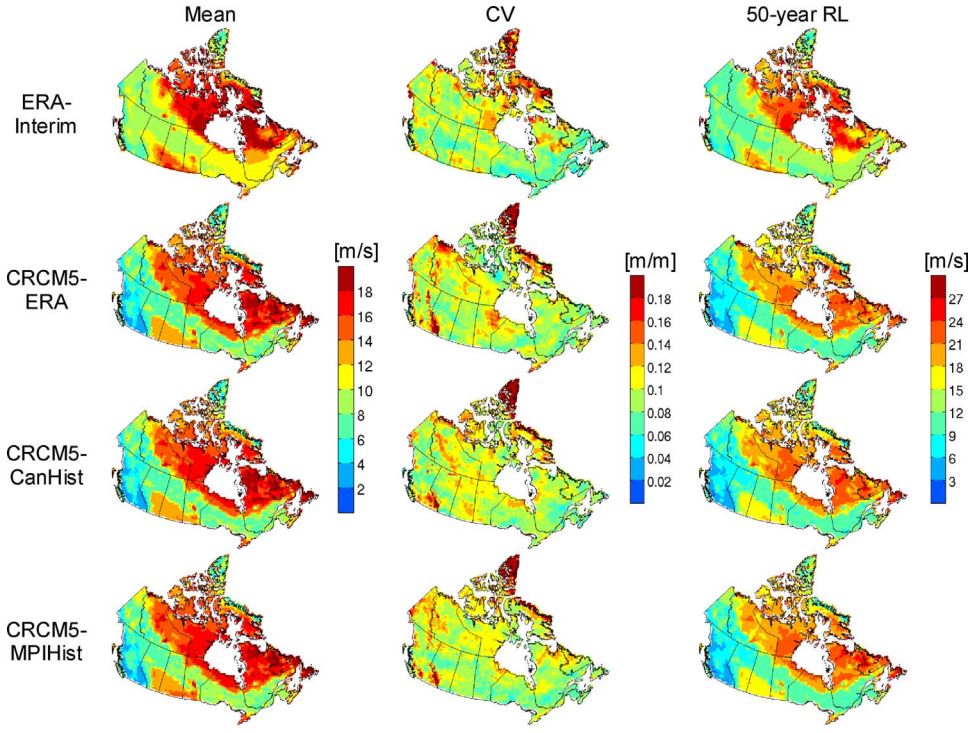

Fig. 3. Mean, coefficient of variation (CV), and 50-year return level (RL) of annual maximum 3-hourly wind speed for ERA-Interim and three CRCM5 simulations for the 1981–2010 period.

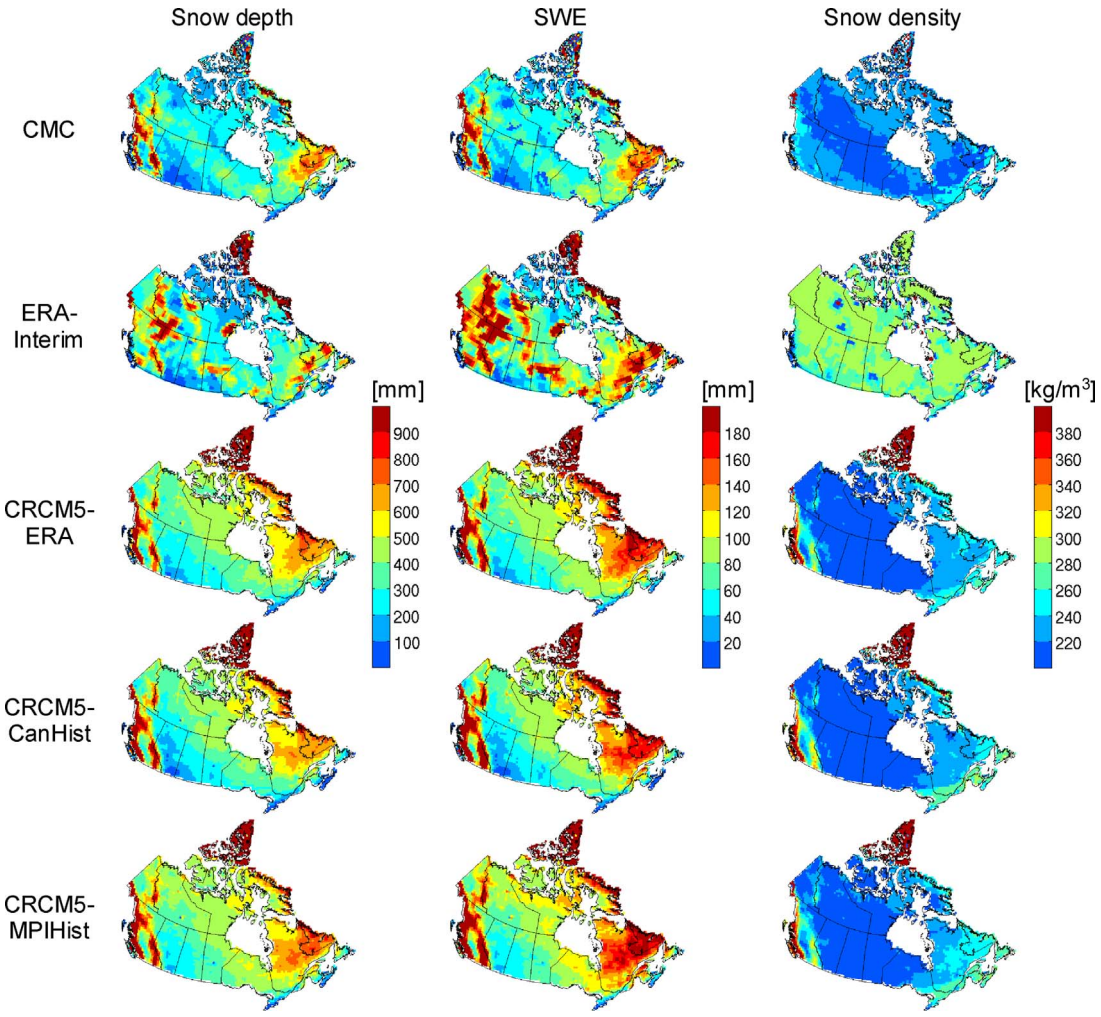

Fig. 4. Mean snow depth, SWE, and snow density for CMC, ERA-Interim, and three CRCM5 simulations for winter (DJFM) for the 1999–2014 period.

2.2. Observed datasets

For validating seasonal and annual mean 3-hourly wind speeds, the homogenized surface (10-m level) wind dataset for Canada (Wan, Wang, & Swail, 2010) for the 1981–2010 period is used. This dataset consists of homogenized monthly mean wind speeds from 156 stations located across Canada; the data starts from 1953 or later. As gridded sub-daily observed dataset for wind speed are not available for Canada, the ERA-Interim reanalysis dataset at 0.75° and 3-hourly resolution for the 1981–2010 period is used for validating annual maximum 3-hourly wind speed. ERA-interim is selected from among the available reanalysis datasets, as it is also used to provide lateral boundary conditions for the CRCM5-ERA simulation. Comparison of ERA-Interim and CRCM5-ERA with observations provides the opportunity to assess added value of downscaling attained with CRCM5.

For validating daily maximum ground snow, Canadian Meteorological Centre (CMC) daily snow depth analysis (Brown & Brasnett, 2015) for Canada for the 1999–2014 period is used. This daily dataset was interpolated to 24 km resolution grids, using a bilinear interpolation scheme from an extensive database of daily snow depth observations from about 8000 U.S. and Canadian cooperative stations (Brasnett, 1999; Brown, Brasnett, & Robinson, 2003). This dataset is up-scaled to the CRCM5 0.44° resolution for this study. Snow water equivalent (SWE), a more comprehensive parameter than snow depth that takes into account snow depth and density, is also validated based on the estimated SWE monthly averages obtained from CMC for the 1999–2014 period. The ERA-Interim reanalysis for the 1999–2014 period is also used for validating annual maximum snow depth and SWE in the three CRCM5 simulations (i.e., CRCM5-ERA, CRCM5-CanHist, and CRCM5-MPIHist).

3. Methodology

Prior to the investigation of future projections, the ability of the CRCM5 in simulating wind and snow is studied. CRCM5-ERA, CRCM5-CanHist, and CRCM5-MPIHist simulated wind speed is evaluated by comparing the magnitude and spatial pattern of seasonal and annual means as well as the annual maximum statistics (i.e., mean, standard deviation, and 50-year return level) with those from observations and ERA-Interim reanalysis for the 1981–2010 period. CRCM5 simulated snow is evaluated by comparing the magnitude and spatial pattern of winter (DJFM) mean snow depth, SWE, and snow density as well as annual maximum daily snow depth statistics (i.e., mean, standard deviation, and expected probable occurrence month) with those of CMC and ERA-Interim reanalysis for the 1999–2014 period. Due to the short record length of the CMC dataset, 50-year return level of annual maximum daily snow depth is not used for CRCM5 evaluation. It is important to note that the annual maximum daily snow depth values are used for the CRCM5 evaluation as daily SWE values are not available in the CMC dataset. Projected changes to snow extremes are analyzed based on daily SWE values, which are available from all CRCM5 simulations.

For all CRCM5 simulations and ERA-Interim reanalysis, annual maximum time series of 3-hourly wind speed and daily mean SWE are

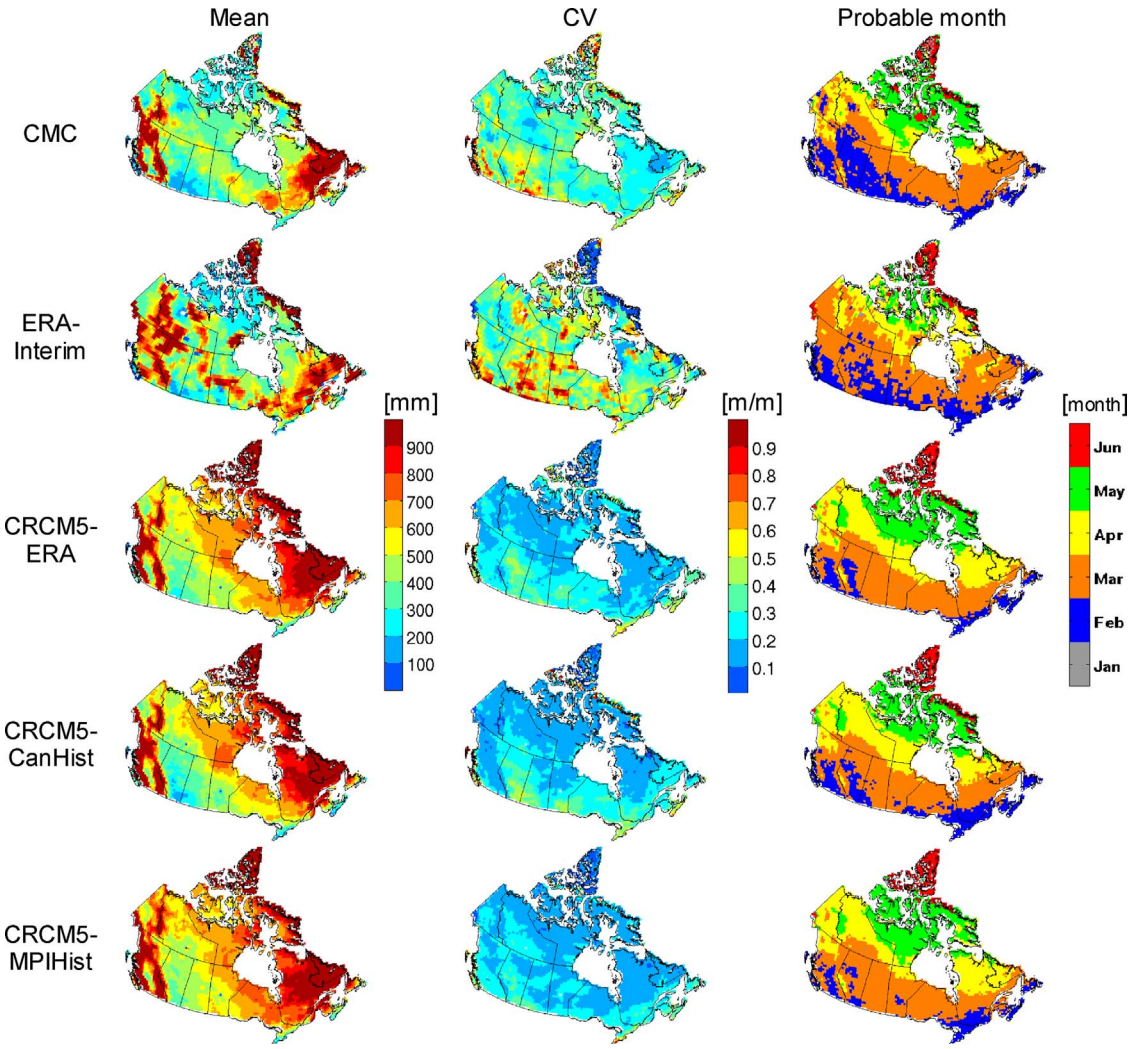

Fig. 5. Mean and CV of annual maximum daily snow depth of CMC, ERA-Interim, and three CRCM5 simulations for the 1999–2014 period. Timing of annual maximum daily snow depth for the same period is presented in the third column.

prepared for all grid points over Canada for the current (1981–2010) and future (2071–2100) periods. Estimation of the selected 50-year return levels of wind speed, wind pressure, SWE, and ground snow load are carried out based on the Gumbel distribution, which is the distribution considered by NBCC for both wind and snow. The Gumbel distribution (Castillo, 2012) is given by,

$$F(x) = \exp(-\exp(-(x - b)/a)), \quad (1)$$

where $F(x)$ denotes the cumulative distribution function, x is the value of the random variable X, and a and b are the scale and location parameters, respectively. The variable X represents either annual maxima of wind speed or SWE. The mean μ_x and standard deviation s_x of X are equal to $b + 0.5772a$ and $a\pi/\sqrt{6}$, respectively. The coefficient of variation (CV) of X is s_x/μ_x. The return value x_T for the T-year return period is given by,

$$x_T = b - a\ln(-\ln(1 - 1/T)). \quad (2)$$

The two parameters are estimated by the method of moments (MOM), which is used by NBCC. The return values of wind pressure q_T and the ground snow load s_T corresponding to the T-year return period are given by,

$$q_T = 0.5\rho\, x_T^2 \quad (3.1)$$

$$s_T = g\, x_T \quad (3.2)$$

where ρ is the air density, and g is gravitational acceleration. Spatial distribution of projected changes to wind speed, wind pressure, SWE, and ground snow load for the future 2071–2100 period with respect to the current 1981–2010 period are presented in the paper. Projected changes to other important wind and snow characteristics such as the directional distribution of annual maximum wind speed, snow density in winter (DJFM), and probable date of annual maximum SWE occurrence are also presented.

4. Results

4.1. Validation

4.1.1. Wind

Fig. 2 shows the spatial distribution of mean annual, summer (JJA), and winter (DJF) wind speeds obtained from observations, ERA-Interim reanalysis, and three CRCM5 simulations, for the 1981–2010 period. Observations show high seasonal and annual mean wind speeds for the Maritimes, northern Plains (i.e., southern parts of Alberta, Saskatchewan, and Manitoba), Hudson Bay region, and northern parts of Quebec. On the other hand, observations show lower wind speed values over western mountainous and boreal forest regions, where surface wind speed is generally small due to high roughness length. The three RCM simulations capture reasonably well the spatial patterns of the observed mean wind speed. The CRCM5-ERA simulation shows slightly

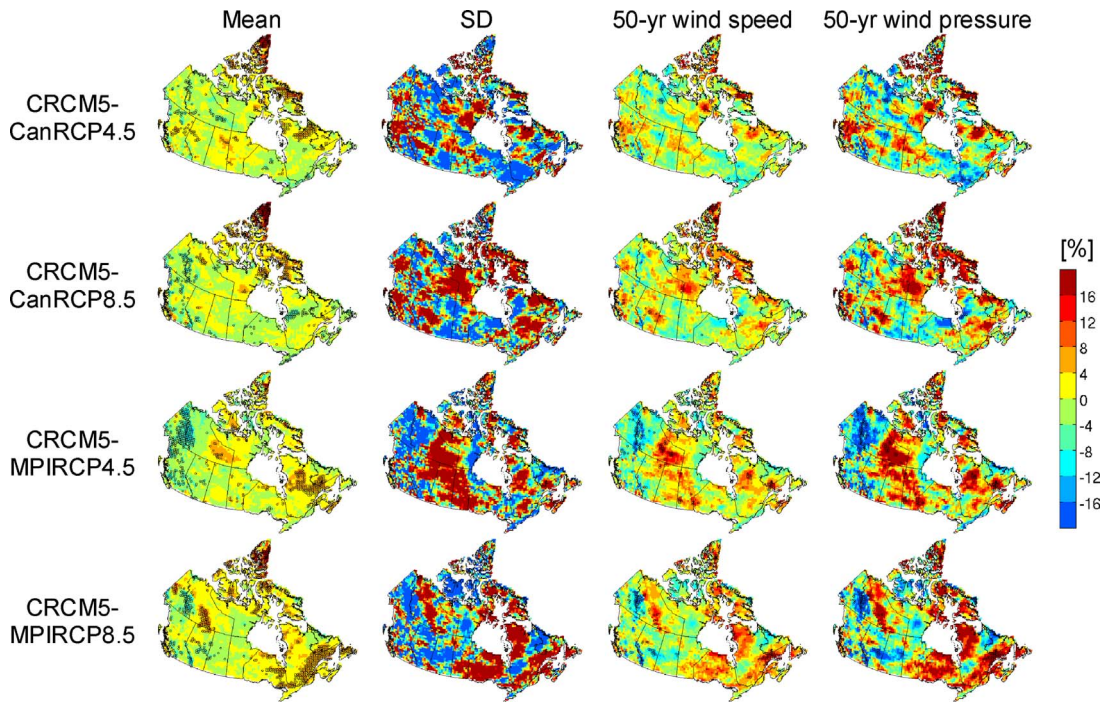

Fig. 6. Projected changes to mean and SD of annual maximum 3-hourly wind speed (columns 1 and 2) and 50-year return level wind speed and wind pressure (columns 3 and 4) for the future 2071–2100 period with respect to the current 1981–2010 period. Grid points are marked by open circles for the mean and 50-year return levels when these variables for the current and future periods are statistically different at the 10% significance level.

better consistency than the ERA-Interim reanalysis with the homogenized station-based dataset for annual mean wind speed; the spatial correlation coefficients are 0.76 and 0.73, respectively. The CRCM5-ERA simulation, however, generally shows lower mean wind speed than ERA-Interim, particularly for the western mountainous and boreal forest regions. The two GCM driven simulations (i.e., CRCM5-CanHist and −MPIHist) show results which are similar to those of CRCM5-ERA, indicating that boundary forcing errors, i.e. the difference between GCM driven and ERA-Interim driven simulations, are generally modest. Spatial distributions of mean spring (MAM) and autumn (SON) wind speeds exhibit similar patterns (not shown).

Fig. 3 shows spatial distributions of mean, CV, and 50-year return level of annual maximum 3-hourly wind speed for ERA-Interim and CRCM5 simulations. The spatial distributions of the mean and 50-year return level of annual maximum 3-hourly wind speed are generally consistent with the contour maps of these variables given in Hong, Mara, Morris, Li, and Ye (2014). It is important to note that the contour maps of Hong et al. (2014) were developed based on hourly wind speed dataset observed at 235 meteorological stations and the ordinary kriging approach. Compared to this, the mean and 50-year return level of annual maximum wind speed of this study are estimated based on 3-hourly time resolution, and therefore are smaller than those of Hong et al. (2014). The CRCM5-ERA simulation shows better agreement with the contour map of Hong et al. (2014) than ERA-Interim for spatial distribution of CV, particularly over the western mountainous regions, and also for spatial distribution of 50-year return level, especially over the northern boundary of boreal forests, possibly indicating the added value of the higher resolution CRCM5 simulations in simulating extreme wind speeds. Again, ERA-Interim generally yields larger values for the mean and 50-year return levels of annual maximum wind speed than the three CRCM5 simulations.

4.1.2. Snow

Fig. 4 shows the spatial distribution of winter (DJFM) mean values of snow depth, SWE, and snow density for CMC, ERA-Interim, and three CRCM5 simulations for the 1999–2014 period. CMC shows high winter snow depth and SWE for western coastal and Rocky Mountain regions as well as for north eastern regions. On the other hand, CMC displays relatively lower winter snow depth and SWE values over the central parts of Canada. The snow density for CMC, which is back-calculated from the snow depth and SWE provided in the figure, shows lower values over the boreal forest and taiga regions than tundra, maritime, and prairie regions, when compared with Sturm, Holmgren, and Liston (1995) and Brown and Mote (2009). The CRCM5 simulations generally agree with the CMC for the spatial distributions of winter snow depth and SWE, although the CRCM5 simulations exhibit higher values for the two variables over the north-eastern parts of Canada (i.e., Hudson Bay region and northern parts of Quebec) regions. Also, the three CRCM5 simulations exhibit lower winter snow density in the prairie region but higher values for the eastern boreal forest and taiga regions than the CMC. The CRCM5 simulations also yield higher winter snow density than CMC over the west coastal regions, which is consistent with the results of Newark, Welsh, Morris, and Dnes (1989) and Hong and Ye (2014). Again, the two GCM driven simulations show similarities with those of CRCM5-ERA for all statistics. ERA-Interim reanalysis, however, shows quite different spatial pattern from the CMC and CRCM5-ERA for the statistics considered, indicating again added value of CRCM5 downscaling to the driving ERA-Interim reanalysis.

Fig. 5 presents spatial distributions of mean, CV, and probable occurrence month of annual maximum daily snow depth for CMC, ERA-Interim, and three CRCM5 simulations for the 1999–2014 period. The 50-year return levels of snow depth are not provided due to short analysis period (i.e. just 16 years) and SWE is not available from CMC at daily time scale. Spatial pattern of annual maximum snow depth for CMC is consistent with the contour maps of Hong and Ye (2014), which were developed based on daily snow depth dataset observed at 549 meteorological stations and the ordinary kriging approach. Again, the three CRCM5 simulations yield higher values for mean annual maximum snow depth over the eastern regions compared to CMC; ERA-Interim reanalysis shows quite different spatial pattern than that of CMC and CRCM5-ERA. The CRCM5 simulations generally yield smaller CV than CMC due to the overestimation of mean snow depth. The

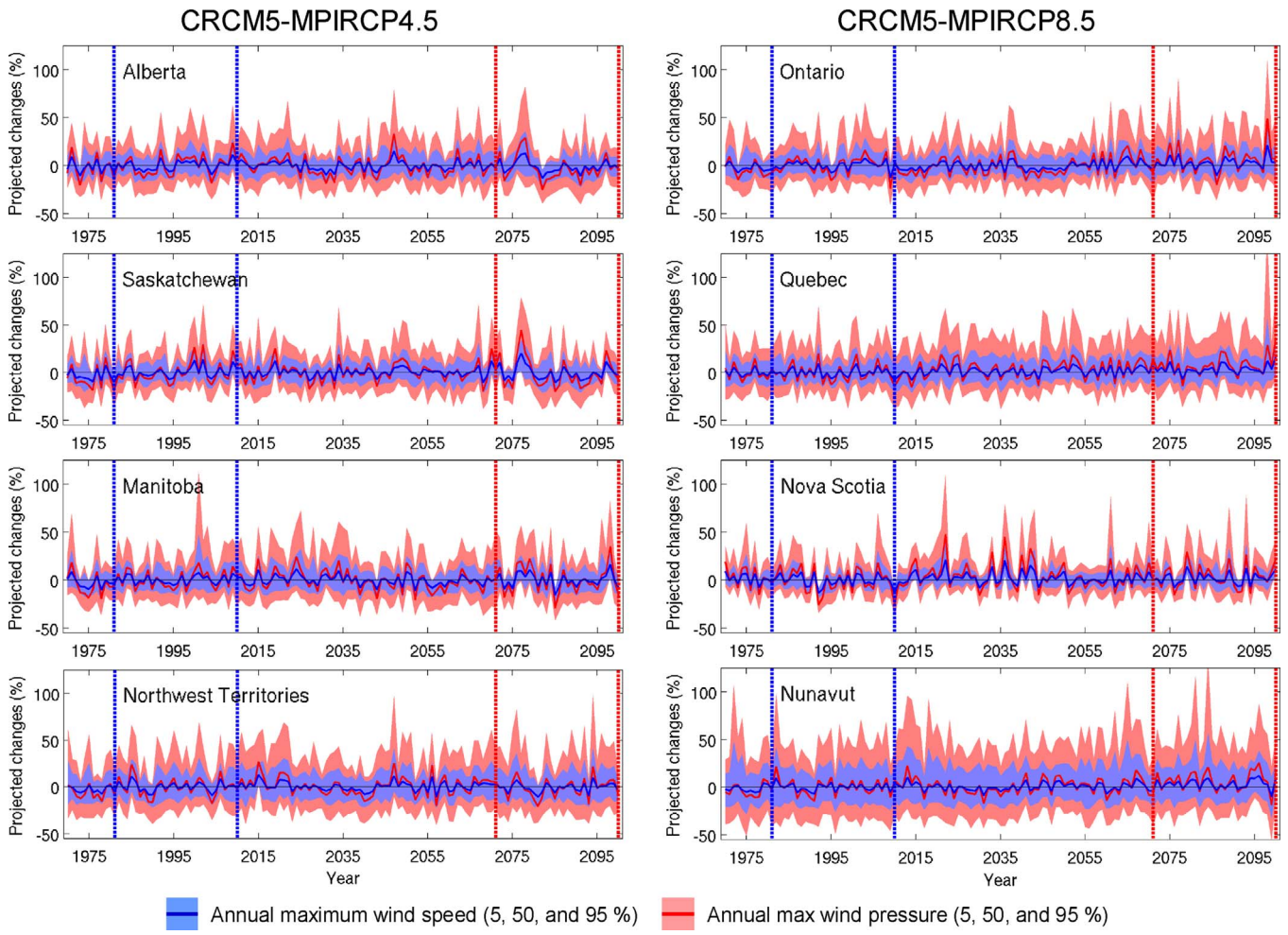

Fig. 7. Projected changes to annual maximum wind speed (blue) and wind pressure (red) with respect to the mean values for the current 1981–2010 period for CRCM5-MPIRCP4.5 (first column) and −MPIRCP8.5 (second column) for selected provinces and territories in Canada. Lower and upper boundaries and solid line respectively represent 5th, 95th, and 50th percentiles of the projected changes from grid points located in the selected provinces or territories. Current and future analysis periods are denoted with blue and red dotted vertical lines.

spatial pattern of the timing of maximum snow depth is similar to the results of Hong and Ye (2014). However, the maximum snow depth in CRCM5 simulations occur later compared to CMC and ERA-Interim, especially over the south-central parts of Canada. This is primarily due to the overestimation of winter precipitation and underestimation of temperature during the winter-spring transition months.

4.2. Projected changes

4.2.1. Extreme wind speed and pressure

Projected changes to the mean and standard deviation (SD) of annual maximum wind speed and 50-year return levels of wind speed and pressure based on four CRCM5 simulations are presented in Fig. 6. Projected changes to the mean and SD display quite different spatial patterns and hence reflect the influence of the driving GCM and emission scenario. Also, there appears to be less coherence among the CRCM5 projections. Projected changes to the SD are larger in magnitude and more variable in space compared to those in the mean values. These results indicate that changes in the spread are generally larger than changes in the mean of the distribution that governs the annual maximum wind speed. The differences of annual maximum wind speed between current and future periods are found statistically insignificant for many cases, when assessed on the basis of the two sample *t*-test at the 10% significance level. It should be noted that changes in future mean sea level pressure (MSLP) in the simulations (not shown) over Canada can increase/decrease intensities of low/high pressure systems situated in those regions such as Aleutian and Icelandic Lows as well as Beaufort High, which in turn lead to changes in future wind speed (Hueging, Haas, Born, Jacob, & Pinto, 2013). Projected changes to the seasonal and annual mean wind speed (not shown) show less spatial variability compared to annual maximum wind speed. Extreme wind speed might be influenced more by regional-scale features associated with instantaneous surface temperature and air pressure gradients and many other similar effects. Projected changes to the 50-year return levels of annual maximum wind speed and pressure show strong spatial consistency with the projected changes in the SD, indicating that change in the inter-annual variability of annual maximum wind speed is the main reasons for changes in the 50-year return levels. General increases in the 50-year return levels for central and eastern Canada are suggested by the end of the 21 st century, mainly due to decrease in future MSLP and associated changes in MSLP gradient. Kumar, Mishra, and Ganguly (2015), based on the CMIP5 multi-model ensemble, also reports increase in the 50-year return levels for the RCP 8.5 scenario.

Spatial and temporal variability of future annual 3-hourly maximum wind speed and wind pressure are investigated further in Fig. 7. This figure shows projected changes to the annual maximum wind speed and wind pressure for CRCM5-MPIRCP4.5 and −MPIRCP8.5 with respect to the current 1981–2010 period for selected provinces and territories of Canada. Four western and four eastern Canadian regions are selected for both CRCM5-MPIRCP4.5 and −MPIRCP8.5. These simulations

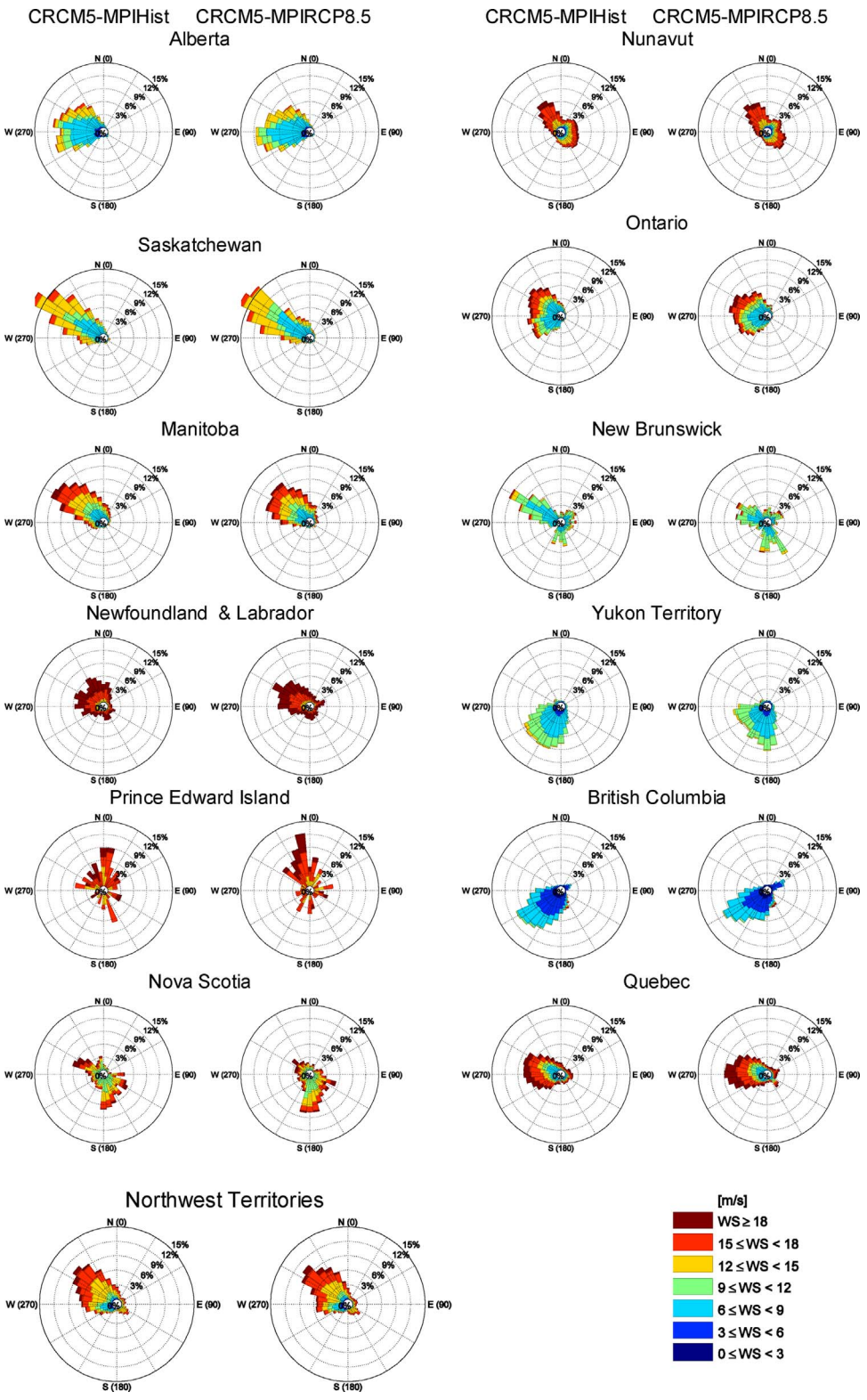

Fig. 8. Directional distributions of annual maximum wind speeds (m/s) for all provinces and territories derived from all related grid cells for the CRCM5-MPIHist simulation (1981–2010) (first column) and CRCM5-MPIRCP8.5 future simulation (2071–2100) (second column). Radial axes show relative frequency of each wind direction (in each 15° sector), and color bins represent wind speed (legend).

exhibit increases in the spatial variability, represented by the range of the blue and red bands, and the inter-annual variability, represented by the fluctuation of the time series of the annual maximum wind speed and wind pressure, for the selected provinces and territories in the future.

Directional distributions of annual maximum 3-hourly wind speed simulated by CRCM5-MPIHist and −MPIRCP8.5 for all provinces and territories are shown in Fig. 8. CRCM5-MPIRCP8.5 exhibits relatively high degree of agreement with the CRCM5-MPIHist for the directional distribution for the selected provinces. The current and future simulations show general westerly directional distribution for the 3-hourly maximum wind speeds, which has been reported based on observed datasets by several studies (e.g., Li and Li (2005), et al. (2016, 2017); et al. (2016, 2017) over Ontario, Hugenholtz and VanVeller (2016) over Alberta, and Bakri, Jackson, and Doherty (2017) over British Colombia). However, there are some notable differences as well. For

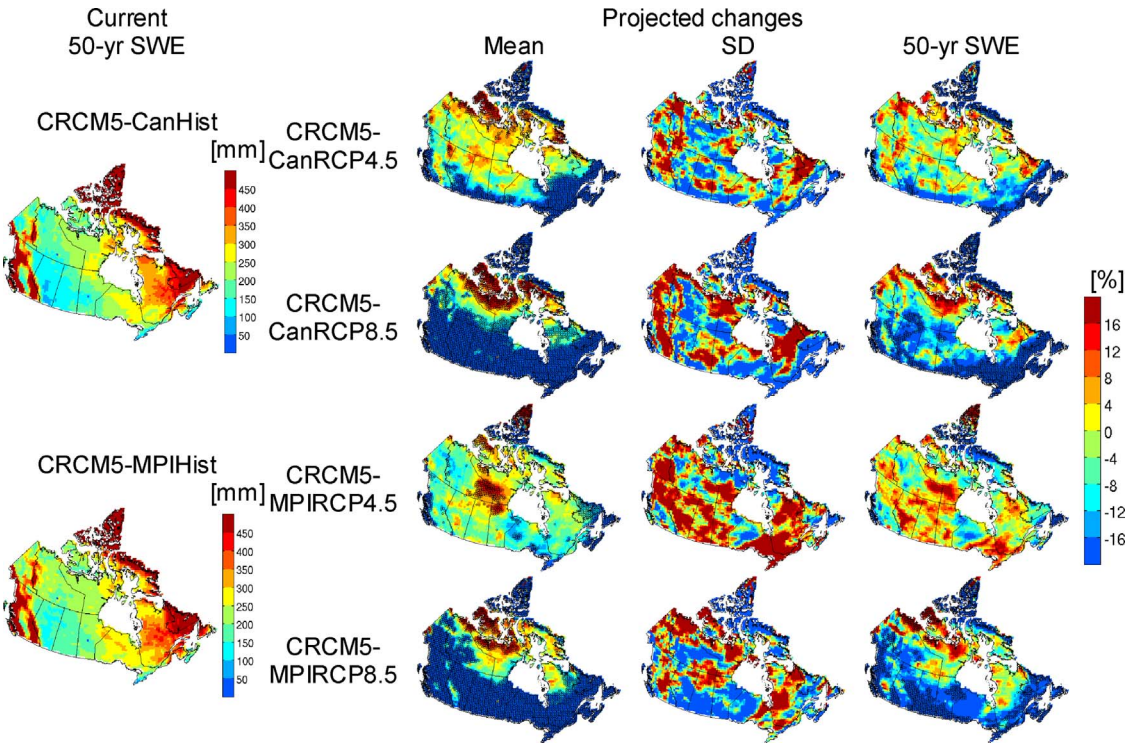

Fig. 9. Projected changes to the mean, SD, and 50-year return level of annual maximum SWE for the 2071–2100 future period with respect to the 1981–2010 current period. Grid points are marked by open circle when the mean and 50-year return level between current and future periods are statistically different at the 10% significance level. The 50-year return levels of annual maximum SWE for the CRCM5-CanHist and CRCM5-MPIHist simulations for the 1981–2010 period are provided in the first column.

instance, future direction of CRCM5-MPIRCP8.5 is more diverse for British Columbia New Brunswick, and Manitoba, but less diverse and more westerly for Alberta, Saskatchewan, Ontario, and Quebec compared to that of CRCM5-MPIHist. Slight changes to the most frequent wind direction between current and future periods are also noticed for Manitoba, Ontario, and Quebec.

4.2.2. Extreme SWE and ground snow load

Projected changes to the mean, SD, and 50-year return level of annual maximum SWE are presented in Fig. 9. The 50-year return levels of annual maximum SWE for the current 1981–2010 period are also shown in this figure. It is important to note that the projected changes (in%) to the mean, SD, and 50-year return level of annual maximum ground snow load are the same as those in the annual maximum SWE due to the linear relationship between the two variables (see Eq. (3.2)). Projected changes to the mean are highly dependent on the RCP emission scenario. The simulations corresponding to the RCP8.5 scenario show significant decreases in the mean values of future annual maximum SWE for most of Canada, except for the high latitude Arctic regions. These changes are due to the future warmer air temperature that lead to delayed snow onset and therefore reduced maximum SWE. Annual maximum SWE and winter precipitation as snowfall could increase in the future for the high latitude regions where winter air temperatures are generally below freezing point. Projected changes to the SD show more variable spatial patterns but larger differences compared to those in the mean. Projected changes to the 50-year return level generally show similar spatial pattern as noted for the mean annual maximum SWE compared to the SD. The simulations evaluated in this study suggest increases in the 50-year return level for some southern and coastal regions along with large increases in the SD, despite decreases in the mean value of annual maximum SWE. It must be noted that CanESM2 generally suggests larger increases in air temperature compared to MPI-ESM (Šeparović et al., 2013), which is also reflected in the CRCM5 simulations (not shown). Consequently, the CRCM5 simulations driven by CanESM2 suggest larger decreases in the annual maximum SWE compared to those driven by MPI-ESM for the southern coastal regions of Canada.

Spatial and temporal patterns of future annual maximum SWE are investigated further in Fig. 10, which shows projected changes (in%) to the annual maximum SWE for selected provinces and territories. The simulations based on the RCP8.5 show significant decreases in annual maximum SWE for British Colombia, Alberta, Saskatchewan, Manitoba, Newfoundland & Labrador, Ontario, Quebec, and New Brunswick for the future 2071–2100 period, although these areas show similar spatial and temporal variability until the middle of the 21 century in many cases. The simulations based on the RCP4.5 show generally larger spatial and temporal variability in annual maximum SWE for the future 2071–2100 period, with slight decreases in the variability for the western and eastern coastal regions. All simulations, however, show increases in both spatial and temporal variability for Yukon and Northwest Territories.

Projected changes to winter (DJFM) snow density and probable date of annual maximum SWE occurrence are presented in Fig. 11. These variables for the current 1981–2010 period are presented in Figs. 4 and 5. Projected changes to the winter snow density are very small, being in the range of −0.2 to 0.2%. However, the spatial distributions are reasonable as they show increases for southern Canada, where warmer air temperatures in future climate could increase wetness of snowpack with increases in overall rainfall frequency and related snow melt in winter (Jeong & Sushama, 2017). All simulations suggest earlier occurrence of annual maximum SWE in the future, due to increases in the future air temperature. The two simulations driven by RCP8.5 yield larger decrease in the date of occurrence compared to those driven by RCP4.5.

5. Summary and discussion

Projected changes to 50-year return levels of wind speed, wind pressure, SWE, and ground snow load over Canada for the future 2071–2100 period are investigated using an ensemble of four CRCM5

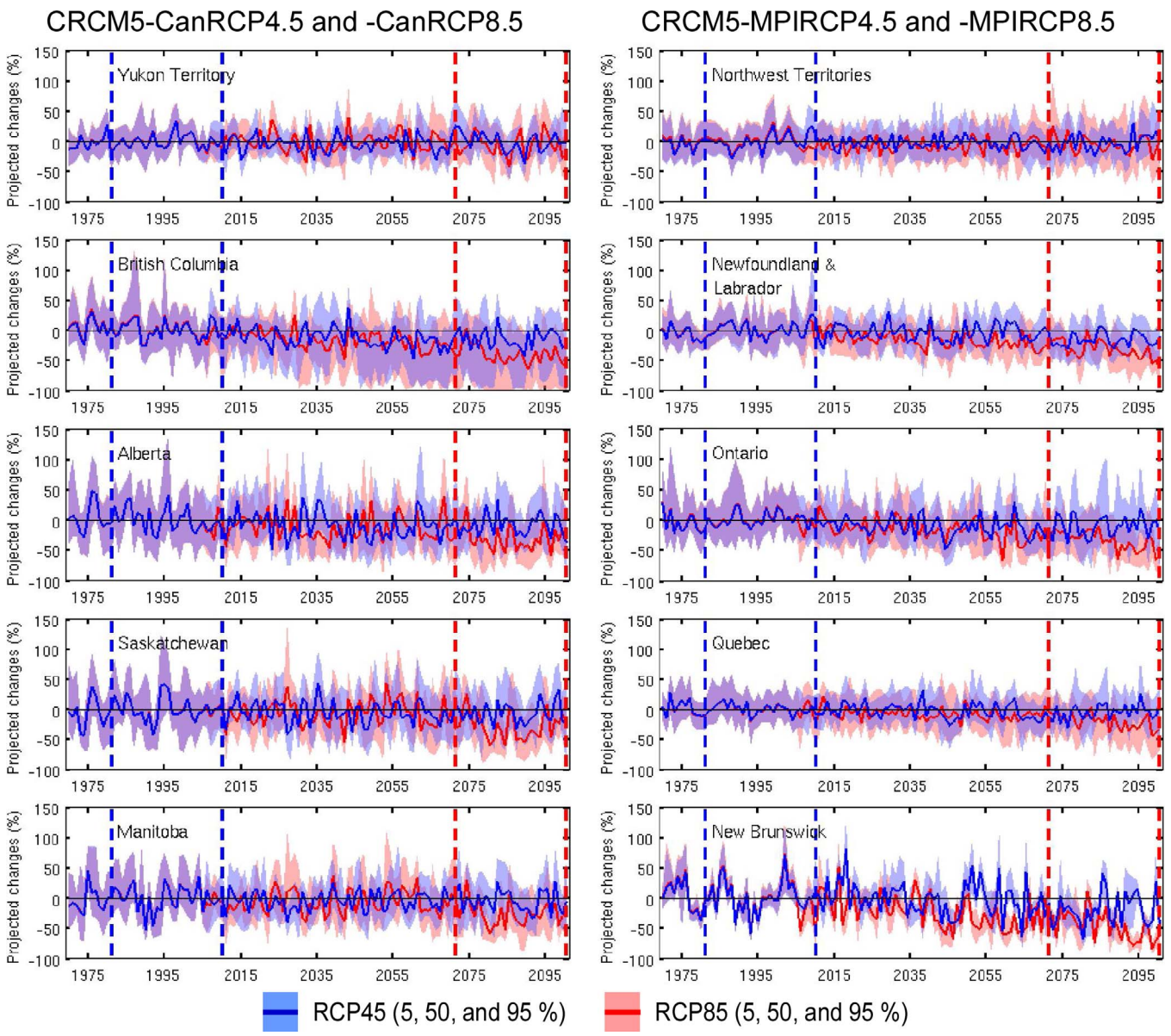

Fig. 10. Projected changes to the annual maximum SWE (and snow load) with respect to the 1981–2010 period mean values for CanESM2 (first column) and MPI-ESM (second column) for selected provinces and territories in Canada. Lower and upper boundaries and solid line represent respectively the 5th, 95th, and 50th percentiles of the projected changes for all relevant grid points. Current and future period analyses are denoted with blue and red dotted vertical lines.

simulations, driven by two GCMs for RCP4.5 and 8.5 scenarios. Evaluation of ERA-Interim driven CRCM5 simulation (CRCM5-ERA) indicates that the regional model is able to reproduce observed magnitudes and spatial patterns of seasonal and annual mean wind speed and winter mean snow depth, SWE, and snow density. The CRCM5-ERA simulation also captures reasonably well the spatial patterns of mean and variance of annual maximum 3-hourly wind speed and daily snow depth. The same simulation also shows some added value with downscaling extreme wind and snow events compared to the driving ERA-Interim reanalysis. The CRCM5 shows modest boundary forcing errors as the two GCM driven simulations (i.e., CRCM5-CanHist and −MPIHist) yield results which are similar to those of CRCM5-ERA for both wind and snow.

The four transient climate simulations suggest quite different spatial patterns of projected changes to the 50-year return levels of wind speed and pressure and hence reflect the influence of the driving GCMs and emission scenarios. Changes in the inter-annual variability of annual maximum wind speed have been identified as the main cause for changes in the 50-year return levels of wind speed and pressure as the simulations considered yield strong spatial consistency between the projected changes to the 50-year return levels and the variability of annual maximum wind speed. Some increases in the 50-year return levels of wind speed and pressure for many grid cells over the eastern, central and Arctic regions of Canada have been noted, although the projected changes are generally less coherent and statistically insignificant. However, comparisons of projected changes to the 50-year return levels between wind speed and pressure illustrates that small increases in extreme wind speed could have significant implications for design and management of buildings and structures, as wind pressure is directly proportional to the square of the wind speed.

The simulations also illustrate that the changes in the future air temperature will be the main contributing factor for changes in extreme ground snow load as the projected changes to the 50-year return levels are highly dependent on the RCP emission scenarios. The simulations based on the RCP8.5, suggest decreasing tendency of the mean of annual maximum SWE as the main cause for decreases in the 50-year return levels of SWE and ground snow load for most parts of southern Canada. The two simulations based on the RCP4.5, suggest that the

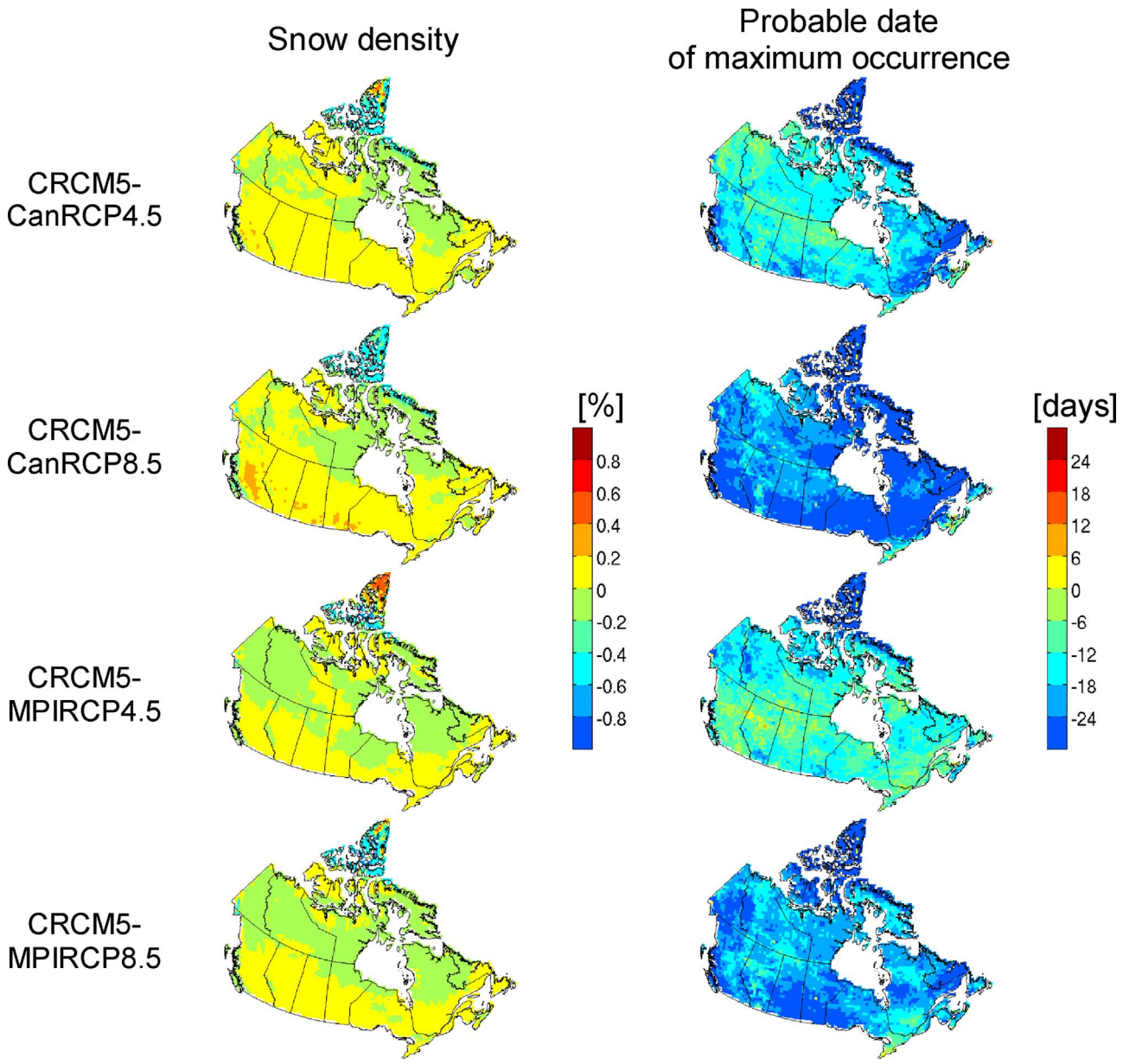

Fig. 11. Projected changes to winter snow density (first column) and probable date of annual maximum SWE occurrence (second column) for the future 2071–2100 period with respect to the current 1981–2010 period.

changes in the inter-annual variability of annual maximum SWE play an important role for changes in the 50-year return levels of SWE and ground snow load. Consequently, the two RCP4.5 simulations yield increases in the 50-year return levels for some southern and coastal regions where they yield increases in the variance of annual maximum SWE, despite decreases in the mean. All simulations suggest earlier date of annual maximum SWE and ground snow load in the range of 10–30 days due to earlier snowmelt as a result of increases in future air temperatures.

The projected changes to extreme wind speed, wind pressure, SWE, and ground snow load derived in this study, based on the high-resolution CRCM5 simulations, will be useful to evaluate detailed regional impacts for many Canadian sectors, particularly for the design and management of buildings and infrastructure. The regional model used in this study generally show reasonable performance in simulating wind and snow. However, underestimation of annual maximum wind speed compared to ERA-Interim and overestimation of annual maximum snow depth compared to CMC have also been noticed. Therefore, some investigations on improving the model performance could be attempted in the future. Projected changes to extreme wind speed and pressure derived based on hourly time-scale resolution simulations is essential for future life cycle cost based design of wind-sensitive structures. In this study, annual maximum wind speed for CRCM5 is derived from 3-hourly simulated data compared to the hourly observations used in the NBCC. Therefore, the model simulated 50-year return levels of wind speed and pressure are basically smaller than those presented in the NBCC. However, it is reasonable to assume that the spatial patterns of projected changes based on 3-hourly simulated data might not be quite different from those based on hourly simulated data. Further investigation is required to verify this point when hourly simulations will become available in the future. As the current study shows that the projected changes are quite dependant on the driving GCMs and emission scenarios, a broader set of simulations including other RCMs and driving GCMs will be necessary to properly evaluate uncertainties in the future projections of wind speed and pressure and ground snow loadings. Moreover, the resolution used in this study did

not allow adequate representation of urban regions. Therefore, it is planned to perform very high resolution CRCM5 simulations with improved urban parameterization to better understand wind speed characteristics for the regions, given the need to incorporate them in the design of urban infrastructure.

Acknowledgements

This research was undertaken within the framework of the Canadian Network for Regional Climate and Weather Processes, funded through the NSERC-CCAR (Natural Sciences and Engineering Research Council-Climate Change and Atmosphere Research) program. All CRCM5 simulations considered in this study were performed on the supercomputer managed by Calcul Québec and Compute Canada.

References

Arora, V. K., Scinocca, J. F., Boer, G. J., Christian, J. R., Denman, K. L., Flato, G. M., et al. (2011). Carbon emission limits required to satisfy future representative concentration pathways of greenhouse gases. *Geophysical Research Letters, 38*, L05805.

Bakri, T., Jackson, P., & Doherty, F. (2017). A synoptic climatology of strong along-channel winds on the Coast of British Columbia, Canada. *International Journal of Climatology, 37*(5), 2398–2412.

Brasnett, B. (1999). A global analysis of snow depth for numerical weather prediction. *Journal of Applied Meteorology, 38*(6), 726–740.

Brown, R. D., & Brasnett, B. (2015). *Canadian Meteorological Centre (CMC) Daily Snow Depth Analysis Data.* Environment Canada, National Snow and Ice Data Center.

Brown, R. D., & Mote, P. W. (2009). The response of northern hemisphere snow cover to a changing climate. *Journal of Climate, 22*(8), 2124–2145.

Brown, R. D., Brasnett, B., & Robinson, D. (2003). Gridded North American monthly snow depth and snow water equivalent for GCM evaluation. *Atmosphere-Ocean, 41*(1), 1–14.

Côté, J., Gravel, S., Méthot, A., Patoine, A., Roch, M., & Staniforth, A. (1998). The operational CMC-MRB global environmental multiscale (GEM) model. Part I: Design considerations and formulation. *Monthly Weather Review, 126*(6), 1373–1395.

Castillo, E. (2012). *Extreme value theory in engineering.* New York: Academic Press.

Cheng, C. S., Li, G., Li, Q., Auld, H., & Fu, C. (2012). Possible impacts of climate change on wind gusts under downscaled future climate conditions over Ontario, Canada. *Journal of Climate, 25*(9), 3390–3408.

Cheng, C. S., Lopes, E., Fu, C., & Huang, Z. (2014). Possible impacts of climate change on wind gusts under downscaled future climate conditions: Updated for Canada. *Journal of Climate, 27*(3), 1255–1270.

Dee, D. P., Uppala, S. M., Simmons, A. J., Berrisford, P., Poli, P., Kobayashi, S., et al. (2011). The ERA-Interim reanalysis: Configuration and performance of the data assimilation system. *Quarterly Journal of the Royal Meteorological Society, 137*(656), 553–597.

Giorgetta, M. A., Jungclaus, J., Reick, C. H., Legutke, S., Bader, J., Böttinger, M., et al. (2013). Climate and carbon cycle changes from 1850 to 2100 in MPI-ESM simulations for the Coupled Model Intercomparison Project phase 5. *Journal of Advances in Modeling Earth Systems, 5*(3), 572–597.

Holt, E., & Wang, J. (2012). Trends in wind speed at wind turbine height of 80 m over the contiguous United States using the North American Regional Reanalysis (NARR). *Journal of Applied Meteorology and Climatology, 51*(12), 2188–2202.

Hong, H. P., & Ye, W. (2014). Analysis of extreme ground snow loads for Canada using snow depth records. *Natural Hazards, 73*(2), 355–371.

Hong, H. P., Mara, T. G., Morris, R., Li, S. H., & Ye, W. (2014). Basis for recommending an update of wind velocity pressures in Canadian design codes. *Canadian Journal of Civil Engineering, 41*(3), 206–221.

Hueging, H., Haas, R., Born, K., Jacob, D., & Pinto, J. G. (2013). Regional changes in wind energy potential over Europe using regional climate model ensemble projections. *Journal of Applied Meteorology and Climatology, 52*(4), 903–917.

Hugenholtz, C. H., & VanVeller, G. A. (2016). Wind hazard in the alpine zone: A case study in Alberta, Canada. *Weather, 71*(2), 27–31.

Hundecha, Y., St-Hilaire, A., Ouarda, T. B. M. J., El Adlouni, S., & Gachon, P. (2008). A nonstationary extreme value analysis for the assessment of changes in extreme annual wind speed over the Gulf of St. Lawrence, Canada. *Journal of Applied Meteorology and Climatology, 47*(11), 2745–2759.

Huziy, O., Sushama, L., Khaliq, M. N., Laprise, R., Lehner, B., & Roy, R. (2013). Analysis of streamflow characteristics over Northeastern Canada in a changing climate. *Climate Dynamics, 40*(7-8), 1879–1901.

IPCC (2012). Managing the risks of extreme events and disasters to advance climate change adaptation. In C. B. Field, V. Barros, T. F. Stocker, D. Qin, D. J. Dokken, K. L. Ebi, M. D. Mastrandrea, K. J. Mach, G.-K. Plattner, S. K. Allen, M. Tignor, & P. M. Midgley (Eds.). *A Special Report of Working Groups I and II of the Intergovernmental Panel on Climate Change*UK, and New York, NY, USA: Cambridge University Press Cambridge 582 pp.

IPCC (2013). Climate Change 2013. In T. F. Stocker, D. Qin, G.-K. Plattner, M. Tignor, S. K. Allen, J. Boschung, A. Nauels, Y. Xia, V. Bex, & P. M. Midgley (Eds.). *The Physical Science Basis. Contribution of Working Group I to the Fifth Assessment Report of the Intergovernmental Panel on Climate Change*United Kingdom and New York, NY, USA: Cambridge University Press Cambridge 1535 pp.

Jeong, D. I., & Sushama, L. (2017). Rain-on-snow events over North America based on two Canadian regional climate models. *Climate Dynamics*. http://dx.doi.org/10.1007/s00382-017-3609-x OnlineFirst,.

Jeong, D. I., Sushama, L., Khaliq, M. N., & Roy, R. (2014). A copula-based multivariate analysis of Canadian RCM projected changes to flood characteristics for northeastern Canada. *Climate Dynamics, 42*(7-8), 2045–2066.

Jeong, D. I., Sushama, L., Diro, G. T., & Khaliq, M. N. (2016). Projected changes to winter temperature characteristics over Canada based on an RCM ensemble. *Climate Dynamics, 47*(5), 1351–1366.

Jeong, D. I., Sushama, L., Diro, G. T., Khaliq, M. N., Beltrami, H., Caya, D., et al. (2016). Projected changes to high temperature events for Canada based on a regional climate model ensemble. *Climate Dynamics, 46*(9-10), 3163–3180.

Kumar, D., Mishra, V., & Ganguly, A. R. (2015). Evaluating wind extremes in CMIP5 climate models. *Climate Dynamics, 45*(1-2), 441–453.

Li, J., & Barker, H. W. (2005). A radiation algorithm with correlated-k distribution. Part I: Local thermal equilibrium. *Journal of the Atmospheric Sciences, 62*(2), 286–309.

Li, M., & Li, X. (2005). Investigation of wind characteristics and assessment of wind energy potential for Waterloo region, Canada. *Energy Conversion and Management, 46*(18), 3014–3033.

McVicar, T. R., Roderick, M. L., Donohue, R. J., Li, L. T., Van Niel, T. G., Thomas, A., et al. (2012). Global review and synthesis of trends in observed terrestrial near-surface wind speeds: Implications for evaporation. *Journal of Hydrology, 416*, 182–205.

NRCC (2015). *National building code of Canada.* Ottawa, Ontario: Institute for Research in Construction, National Research Council of Canada.

Newark, M. J., Welsh, L. E., Morris, R. J., & Dnes, W. V. (1989). Revised ground snow loads for the 1990 National Building Code of Canada. *Canadian Journal of Civil Engineering, 16*(3), 267–278.

Peacock, S. (2012). Projected twenty-first-century changes in temperature, precipitation, and snow cover over North America in CCSM4. *Journal of Climate, 25*(13), 4405–4429.

Romanić, D., Ćurić, M., Jovičić, I., & Lompar, M. (2015). Long-term trends of the 'Koshava'wind during the period 1949–2010. *International Journal of Climatology, 35*(2), 288–302.

Romanić, D., Hangan, H., & Ćurić, M. (2016). Wind climatology of Toronto based on the NCEP/NCAR reanalysis 1 data and its potential relation to solar activity. *Theoretical and Applied Climatology*. http://dx.doi.org/10.1007/s00704-016-2011-7.

Romanić, D., Rasouli, A., & Hangan, H. (2017). Urban wind resource assessment in changing climate: Case study. *Wind Engineering, 41*(1), 3–11.

Šeparović, L., Alexandru, A., Laprise, R., Martynov, A., Sushama, L., Winger, K., et al. (2013). Present climate and climate change over North America as simulated by the fifth-generation Canadian regional climate model. *Climate Dynamics, 41*, 3167–3201.

Steenbergen, R. D., Koster, T., & Geurts, C. P. (2012). The effect of climate change and natural variability on wind loading values for buildings. *Building and Environment, 55*, 178–186.

Sturm, M., Holmgren, J., & Liston, G. E. (1995). A seasonal snow cover classification system for local to global applications. *Journal of Climate, 8*(5), 1261–1283.

Vautard, R., Cattiaux, J., Yiou, P., Thépaut, J. N., & Ciais, P. (2010). Northern Hemisphere atmospheric stilling partly attributed to an increase in surface roughness. *Nature Geoscience, 3*(11), 756–761.

Verseghy, D. (2009). *CLASS the Canadian land surface scheme (version 3.4), Tech. Rep.* Environment Canada: Climate Research Division, Science and Technology Branch107.

Verseghy, D. (2012). *CLASS-The Canadian Land Surface Scheme (Version 3.6). Tech. Rep.* Environment Canada: Climate Research Division, Science and Technology Branch179.

Wan, H., Wang, X. L., & Swail, V. R. (2010). Homogenization and trend analysis of Canadian near-surface wind speeds. *Journal of Climate, 23*(5), 1209–1225.